

pubs.acs.org/JPCC Article

Computing the Tantalum-Nitrogen Phase Diagram at High Pressure and High Temperature

Hanof Alkhaldi and Peter Kroll*



Cite This: J. Phys. Chem. C 2020, 124, 22221-22227

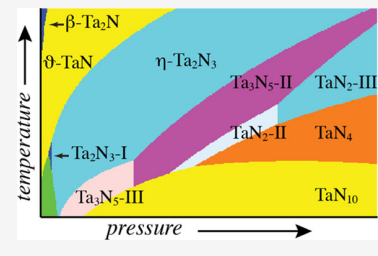


ACCESS I

Metrics & More

Article Recommendations

ABSTRACT: We investigate the pressure—temperature phase diagram of the tantalum—nitrogen system through a combination of density functional theory computations and thermodynamic calculations. Accounting for the chemical potential of nitrogen at high pressure and high temperature, we obtain a Gibbs energy surface for every Ta—N phase in the pressure—temperature space. Combining the data yields a coherent stability map that identifies the one most favorable Ta—N structure at given *p*, *T* conditions in the presence of excess nitrogen. Slices through the phase diagram at constant pressure or constant temperature are used to examine the manifold of competing structures and locate optimum conditions with maximum driving force for successful syntheses. We rationalize high-pressure



experiments that synthesized new Ta-N polymorphs and predict the temperature and pressure conditions necessary to synthesize $Ta_2N_2(N_2)$ and Ta_2N_8 .

INTRODUCTION

Progress in experimental high-pressure/high-temperature (HPHT) techniques over the last 2 decades yielded many new transition-metal nitrogen (TM-N) compounds. These include nitrides,² pernitrides,^{3,4} mixed nitride-pernitrides,⁵ compounds comprising complex polyatomic nitrogen anions, and compounds with extended anionic nitrogen chains -- just to provide a few examples from a continuously growing list. There are two major experimental pathways toward novel TM-N compounds at HPHT. One combines reactants, elements, or pre-existing TM-N compounds, with an excess of nitrogen loaded in diamond-anvil cells (DAC), and applies laser heating.⁸⁻¹⁰ The other approach starts with solid-state compounds, for instance, a low-pressure polymorph or a nitrogen-rich single-source precursor, potentially in combination with a nitrogen-rich reactant. This approach can be applied either in a DAC or in a large-volume press, e.g., a multianvil apparatus,⁵ after the initial compression temperature is raised to usually 1500 K and higher to initiate reactions between the reactants and nitrogen, or to induce phase transformations and decompositions. Though it is thinkable that stronger "kinetic control" may be possible at lower temperatures, such methods are still in their nascent stage.

Experimental studies have been motivated or examined by computational efforts, and synergy between different approaches drives new explorations. Advances in computer resources and suitable algorithms and programs [Ab initio random structure searching (AIRSS),¹¹ Universal Structure Predictor: Evolutionary Xtallography (USPEX),¹² XTALOPT,¹³ crystal structure prediction via particle swarm optimization (CALYPSO)¹⁴] make high-throughput calculations feasible to search for structures, and it appears that far

more new TM-N structures have been envisioned than have been realized in experiments. With nitrogen as one reactant during synthesis, the fidelity of computational predictions depends on how well the chemical potential of nitrogen is assessed at high temperature and high pressure. ¹⁵⁻¹⁷ We recently provided intelligible data for the chemical potential change of molecular nitrogen relative to its enthalpy at various temperature and pressure conditions. ¹⁸ Here, we apply the combination of thermochemical data with first-principles calculations to explore the pressure—temperature phase diagram of tantalum—nitrogen.

Tantalum—nitrogen compounds obtained in experiments include crystalline structures of Ta_2N , TaN, Ta_3N_6 , Ta_4N_5 , Ta_2N_3 , and Ta_3N_5 . Much computational work has been devoted to identify additional Ta-N structures that can be obtained in high-pressure experiments. Our early assessment of the pressure—temperature phase diagram of nitrogenrich tantalum nitride addressed a phase boundary between TaN and Ta_3N_5 at high temperature and high pressure. Motivated by this work, three experimental endeavors were reported. Zerr et al. used crystalline Ta_3N_5 as the starting material in a multianvil apparatus (large-volume press). At 11 GPa and 1773 K and at 20 GPa and 1973 K, they obtained η- Ta_2N_3 with marginal contamination with oxygen. Friedrich et

Received: May 8, 2020
Revised: August 7, 2020
Published: September 11, 2020





Table 1. $\Delta\mu(T, p_{N_1})$ (in eV/atom) of Nitrogen, Treating Nitrogen as Perfect Gas, $\gamma = 1$ (ln $\gamma = 0$)

| $\Delta\mu(T,p_{ m N_2})$ | 0 GPa | 20 GPa | 40 GPa | 60 GPa | 80 GPa | 100 GPa | 120 GPa | 140 GPa |
|---------------------------|-------|--------|--------|--------|--------|---------|---------|---------|
| 1500 K | -1.23 | -0.89 | -0.85 | -0.82 | -0.80 | -0.79 | -0.78 | -0.77 |
| 2000 K | -1.72 | -1.27 | -1.21 | -1.18 | -1.15 | -1.13 | -1.12 | -1.10 |
| 2500 K | -2.24 | -1.67 | -1.60 | -1.55 | -1.52 | -1.50 | -1.48 | -1.46 |
| 3000 K | -2.77 | -2.09 | -2.00 | -1.95 | -1.91 | -1.88 | -1.86 | -1.84 |

Table 2. $\Delta \mu(T, p_{N_2})$ (in eV/atom) of Nitrogen within the Moderate Extrapolation

| $\Delta\mu(T,p_{ m N_2})$ | 0 GPa | 20 GPa | 40 GPa | 60 GPa | 80 GPa | 100 GPa | 120 GPa | 140 GPa |
|---------------------------|-------|--------|--------|--------|--------|---------|---------|---------|
| 1500 K | -1.21 | -0.21 | -0.16 | -0.13 | -0.11 | -0.10 | -0.08 | -0.07 |
| 2000 K | -1.71 | -0.61 | -0.54 | -0.51 | -0.48 | -0.46 | -0.45 | -0.44 |
| 2500 K | -2.22 | -1.02 | -0.94 | -0.90 | -0.87 | -0.84 | -0.82 | -0.81 |
| 3000 K | -2.76 | -1.45 | -1.36 | -1.31 | -1.27 | -1.24 | -1.22 | -1.20 |

Table 3. $\Delta \mu(T, p_{N_2})$ (in eV/atom) of Nitrogen within the Progressive Extrapolation

| $\Delta\mu(T,p_{ m N_2})$ | 0 GPa | 20 GPa | 40 GPa | 60 GPa | 80 GPa | 100 GPa | 120 GPa | 140 GPa |
|---------------------------|-------|--------|--------|--------|--------|---------|---------|---------|
| 1500 K | -1.21 | 0.09 | 0.42 | 0.62 | 0.76 | 0.87 | 0.96 | 1.04 |
| 2000 K | -1.71 | -0.29 | 0.05 | 0.26 | 0.41 | 0.53 | 0.63 | 0.71 |
| 2500 K | -2.22 | -0.69 | -0.33 | -0.12 | 0.04 | 0.16 | 0.26 | 0.35 |
| 3000 K | -2.76 | -1.11 | -0.74 | -0.51 | -0.35 | -0.22 | -0.12 | -0.03 |

al. performed experiments in a laser-heated DAC starting with tantalum embedded in excess nitrogen. 25 They synthesized η -Ta2N3 in several experiments between 9 and 27 GPa and temperatures estimated to be between 1600 and 2000 K. Salamat et al. loaded a diamond-anvil cell (DAC) with an amorphous polymeric N-rich Ta-N precursor, which at ambient pressure could also be crystallized to yield the ambient pressure modification Ta₂N₅-I. ²⁶ After increasing the pressure to 20 GPa and laser heating at 1500-2000 K, they obtained a phase assemblage, which was analyzed to consist of Ta₃N₅-II and the U₃Se₅-type of Ta₃N₅ together with small amounts of η -Ta₂N₃ and ε -N₂.

In this contribution, we will first outline the computational approach and then present computed pressure-temperature phase diagrams for the tantalum-nitrogen system that help in identification of thermodynamically stable phases and their respective stability field. We then provide slices through the phase diagram at constant pressure and at constant temperature, respectively, that help experimentalists to locate conditions of maximum driving force for successful syntheses. We then contrast convex-hull data based on formation enthalpy and formation Gibbs energy and close with a discussion.

COMPUTATIONAL METHOD

Calculations of total energy and volume were done within the density functional theory (DFT) as implemented in Vienna ab initio simulation package (VASP).^{27–30} We used pseudopo tentials based on the projector-augmented-wave (PAW)31,32 method together with the strongly constrained and appropriately normed (SCAN) semilocal density functional.³³ Brillouin zone integration happened for each structure through appropriate k-point meshes with grid sizes smaller than 0.03 Å⁻¹. All reported results rely on a plane wave cutoff energy of 500 eV, and forces were converged to better than 1 meV/Å, yielding energy and enthalpy differences between structures converged to better than 1 meV per atom.

For structural explorations, we first computed the wealth of previously reported structures in the Ta-N system. $^{19-23}$ We then augmented the database by structures attained via an evolutionary algorithm (USPEX¹²) as well as through a random structure search (AIRSS¹¹). Searches were performed at 40, 80, 120, and 160 GPa (and T = 0 K) with up to 20 and more atoms in a simulation cell. We also added models originally received for different transition-metal nitride compounds to our search. 34,35 Overall, two previously unreported polymorphs (Ta₃N₅-III and TaN₂-II, described below) emerged from this approach.

To acquire enthalpy-pressure (H-p) data, we proceed as described previously:³⁶ for a given structure, we optimize its structural parameters at a given volume. We then vary the volume systematically, and for each new volume, we optimize the structure and compute its energy. The resulting E-V data yields pressure p by numerical differentiation, $p = -\partial E/\partial V$, and we compute the enthalpy by H = E + pV. For solid-state reactions, reaction Gibbs energies $\Delta G = \Delta H - T \cdot \Delta S$ are well approximated by reaction enthalpies ΔH because entropy contributions to ΔG are usually small in comparison to changes of ΔH within a few GPa. A similar argument is made in light of a possible temperature dependency of enthalpies: heat capacities of solid reactants and products at high temperatures do not differ to an extent that exceeds the changes of ΔH within a few GPa.

Once a gaseous or fluid component participates in the reaction, however, the impact of temperature is important and will often determine the outcome of an experiment. Therefore, in reactions involving nitrogen, its chemical potential μ (Gibbs molar energy) and its increment $\Delta \mu$ relative to molar enthalpy must be taken into consideration at any temperature and pressure. In previous works, we specified approaches to quantify $\Delta \mu$ at high temperatures and high pressures. ¹⁶ Besides perfect gas behavior, we provided a moderate and more progressive extrapolation for the fugacity of nitrogen under these conditions. In Tables 12-3, we summarize the results for the chemical potential increment $\Delta \mu(T, p_{N_2})$ of nitrogen.¹⁸ Note that the data at 0 GPa corresponds to NIST tabulated data,³⁷ with only small variations for the two extrapolations due to their particular functional form. Detailed discussions of the approach and applications to various systems can be found in refs 16 and 18.

Using the computed enthalpies of all tantalum-nitrogen compounds, including tantalum and molecular nitrogen (ε - N_2), together with the chemical potential increment $\Delta \mu(T,$ $p_{\rm N_2}$) of nitrogen, we can now assess the Gibbs energy for each system, locate phase boundaries ($\Delta G = 0$), and identify the thermodynamically most stable phase with its structure in the temperature-pressure phase diagram. Within this approach, "thermodynamic stability" refers to a system with excess nitrogen and with pressure equal to the partial pressure of nitrogen. The temperature-pressure conditions we explore are typically realized in DAC experiments using nitrogen as pressure medium together with laser heating. To display phase diagrams, we chose the temperature 1000-4000 K and the pressure range 0-140 GPa. Throughout, the source for excess nitrogen (our reference) is molecular nitrogen (ε -N₂). It is known that polymeric nitrogen forms at 110 GPa and 2000 K.10 Thus, going beyond these pressure and temperature conditions neglects a potential transformation into the extended form of nitrogen. A computational assessment of the phase boundaries between molecular and polymeric nitrogen has recently been given elsewhere.¹⁸

RESULTS

Combining first-principles computations with thermodynamic calculations, we compute the pressure-temperature (p, T)phase diagram for the tantalum-nitrogen system. Three diagrams resulting from using the three different approximations for the chemical potential of nitrogen are shown in Figure 1. Each diagram displays the thermodynamically most stable Ta-N phase at the given p, T-conditions in the presence of excess nitrogen.

At low pressure and low temperature, the computed Ta-N phase diagrams display the structure of Ta₃N₅-I, the lowest energy orthorhombic polymorph of Ta₃N₅ with space group symmetry Cmcm (no. 62).³⁸ At higher temperature, hexagonal ϑ -TaN (P-6m2 (187)) emerges, and above 3000 K, we find β -Ta₂N (P31m (157)). Within the SCAN functional, we compute the rival mononitride ε -TaN with a slightly higher energy at zero pressure than ϑ -TaN. Since the latter has a more favorable pressure behavior, it is the only TaN structure stable in the phase diagram.

A significant part of the phase diagram is then occupied by η -Ta₂N₃, the orthorhombic U₂S₃-type structure (Pnma (62)).²⁴ Interestingly, our calculations yield a small stability range of tetragonal Ta₂N₃ (P-4m2 (115)) below 5.8 GPa as well, consistent in all approximations for the chemical potential of nitrogen. This phase was proposed to precede η -Ta₂N₃ at lower pressures.

Increasing the pressure further yields two more structures of Ta₃N₅. Above 38 GPa, the previously predicted U₃Te₅-type of Ta₃N₅-II (*Pnma* (62)) will appear. Yet another orthorhombic structure, Ta₃N₅-III (Pmmn (59)), is intermediate between the ambient pressure modification Ta₃N₅-I and the highpressure modification Ta₃N₅-II. Ta₃N₅-III appears above 1000 K only when using the moderate or progressive extrapolation. Since Ta_3N_5 -III borders to η - Ta_2N_3 at higher temperatures,

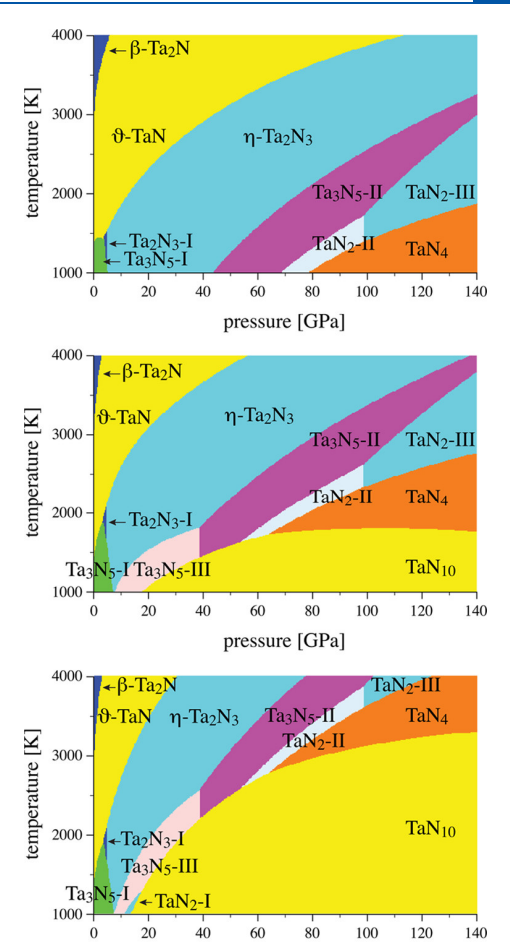


Figure 1. Tantalum-nitrogen pressure-temperature phase diagrams computed by combining first-principles (SCAN functional) and thermodynamic calculations. The pressure axes refer to the partial pressure of nitrogen $(p(N_2))$. For the fugacity of nitrogen, we use (top) the perfect gas approximation, (middle) the moderate, and (bottom) the progressive extrapolation formula. The structures of the individual phases are explained in the text.

pressure [GPa]

temperature has a significant impact on a potential synthesis of Ta₃N₅-III, as will be addressed in the discussion below.

At even higher pressures, we observe two polymorphs with composition TaN_2 : monoclinic $(P2_1/c (14)) TaN_2$ -II followed at 98 GPa by orthorhombic (Cmca (64)) TaN2-III. Our labels (II and III) have been chosen to allow for a low-pressure monoclinic polymorph TaN_2 -I (C2/m (12)), which occurs only in the phase diagram computed using the progressive extrapolation formula for the chemical potential change of nitrogen. Polymorphs I and III have been proposed previously for TaN2 and NbN2. 23,35 All three TaN2 structures are mixed nitride-per-nitrides, $TaN_2 == Ta_2N_2(N_2)$. Two more phases with high nitrogen content emerge at high pressures. Monoclinic TaN₄ (P2₁/c (14)) displays a finite chain of nitrogen atoms forming a complex N₈¹⁰⁻-anion; hence, TaN₄ == $Ta_2(N_8)$. This structure has been proposed previously as well. 23,35 Finally, we include orthorhombic TaN₁₀ (Immm (71)) that displays infinite chains of nitrogen together with enclosed N2 molecules. This structure has been predicted for HfN₁₀ already.³⁵

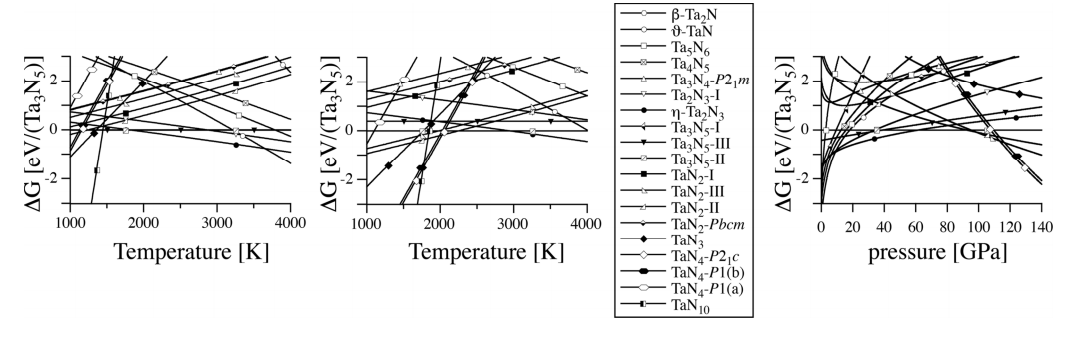


Figure 2. (Left side of legend) Relative Gibbs energy versus temperature, $\Delta G - T$, of Ta-N phases in excess nitrogen at 40 and 80 GPa, respectively. (right side of the legend) relative Gibbs energy versus pressure, $\Delta G - p$, of Ta-N phases in excess nitrogen at 2500 K. Symbols in the respective diagrams refer to the structures listed in the boxed legend. Note that in each diagram energy refers to an overall composition Ta₃N₅. For all phases, thus, a proper amount of molecular nitrogen is added (or subtracted), e.g., $11/2 \cdot Ta_2N_3 + 1/4 \cdot N_2 \rightarrow Ta_3N_5$.

Among the structures that do not have a stability field in the computed phase diagram are the nitrides ε-TaN, Ta₅N₆, Ta_4N_5 , Ta_3N_4 , and TaN_3 . This is in part due to the SCAN functional chosen in our work, but also to the conditions stated: in the presence of excess nitrogen below 140 GPa and temperatures above 1000 K, these phases are not thermodynamically stable.

Phase diagrams as displayed in Figure 1 are essential for material synthesis and for understanding phase relations. We need to keep in mind, however, that they display only the minimum Gibbs energy structure at a given p, T-condition. The diagrams do not show—for instance—competitive structures, some of which may have a kinetic advantage during synthesis. It is also quite difficult to provide error bars showing uncertainties in phase boundaries. These can be large in cases where the relative slopes of the intersecting the Gibbs energy landscapes are shallow rather than steep. To provide more insight into the phase diagram, and ultimately to provide support for experimentalists, we display relative Gibbs energy versus temperature data $(\Delta G - T)$ and relative Gibbs energy versus pressure data $(\Delta G - p)$ for tantalum-nitrogen phases. We will restrict this discussion to the moderate extrapolation for the chemical potential of nitrogen. Our recent comparison of experimental and computed data in the titanium-nitrogen system indicates that its outcomes are closest to experimental observations.18

In laser-heated DAC experiments targeting the synthesis of new nitrides, the reactant is typically embedded in nitrogen as pressure medium. Thereafter, the pressure is increased to a desired level, and then laser heating is applied to increase the temperature. We have this experimental procedure in mind for the ΔG –T diagrams at 40 and 80 GPa shown in Figure 2. These are "slices" through the phase diagram of Ta-N phases in the presence of excess nitrogen at constant pressure. Each line represents the Gibbs energy of a system comprising a structure with a given composition plus appropriate amounts of nitrogen relative to the Gibbs energy of Ta₃N₅-II. Assuming equilibrium to be established, the system with the lowest Gibbs energy (here ΔG) will form at the respective temperature. Phase boundaries in the phase diagram shown in Figure 1 (middle), therefore, will align with line crossings in the $\Delta G - T$ graphs shown in Figure 2. At 40 GPa, we have the sequence:

$$TaN_{10} \xrightarrow{1450 \text{ K}} Ta_3N_5\text{-II} \xrightarrow{1850 \text{ K}} \eta\text{-Ta}_2N_3 \xrightarrow{3650 \text{ K}} \vartheta\text{-TaN}$$

At 80 GPa, we compute

$$TaN_{10} \xrightarrow{1800 \text{ K}} TaN_4 \xrightarrow{2000 \text{ K}} TaN_2\text{-II} \xrightarrow{2250 \text{ K}} Ta_3N_5\text{-III} \xrightarrow{2950 \text{ K}} \eta\text{-Ta}_2N_3$$

The data is easily used to quantify the driving force (ΔG) for a conversion and to locate "optimum" conditions for a synthesis where ΔG is maximized. For instance, at 80 GPa, the Ta₃N₅-II structure will be favorable between 2250 and 2950 K. Its thermodynamic stability is optimal at a temperature of 2500 K, favored by about 0.18 eV per Ta₃N₅ over its closest competitors TaN_2 -I and η - Ta_2N_3 . In addition, the graphs allow fair estimates about the impacts of structural defects or systematic errors in the computational approach on reaction outcomes.

In a similar way, we show relative Gibbs energies at constant temperature as a function of pressure, $\Delta G - p$, for tantalum nitrogen phases. For a temperature of 2500 K, this is shown in Figure 2 on the right side. We find the sequence

$$\begin{array}{c} \vartheta\text{-TaN} \xrightarrow{9 \text{ GPa}} \eta\text{-Ta}_2\text{N}_3 \xrightarrow{61 \text{ GPa}} \text{Ta}_3\text{N}_5\text{-II} \xrightarrow{93 \text{ GPa}} \text{TaN}_2\text{-II} \\ \xrightarrow{98 \text{ GPa}} \text{TaN}_2\text{-III} \xrightarrow{116 \text{ GPa}} \text{TaN}_4 \end{array}$$

Once again, the data can be used to identify the best conditions for synthesizing a particular structure. While the thermodynamic stability of Ta₃N₅-II at 2500 K extends from 61 to 93 GPa, the largest ΔG of about 0.18 eV per Ta₃N₅ relative to competitors (TaN₂-I and η -Ta₂N₃) is found at 81

A different concept invoked for discussing the thermodynamic stability of compounds is that of a "convex hull". A convex hull is a set of phases, all of which have positive reaction energies for a decomposition into any combination of neighboring phases. It is founded on the formation energies of compounds and can be worked out from experimental as well as computational data. Convex hulls are frequently used in chemistry to display thermodynamic stability even in a broader context, e.g., Frost-Ebsworth diagrams in electrochemistry. In high-pressure science, however, these are typically composition-formation enthalpy convex hulls constructed from the results obtained at 0 K. Therefore, they address the relative stabilities of compounds under constant composition but have only limited applicability in predicting the thermodynamic stable phases in the presence of excess nitrogen at elevated temperature. In other words, they predict the outcome of a solid-state reaction (e.g., $TaN + Ta_3N_5 \rightarrow 2 Ta_2N_3$) but cannot address simultaneous competing reactions with nitrogen (e.g., $2 \text{ Ta}_2 \text{N}_3 \rightarrow 4 \text{ TaN} + \text{N}_2 \text{ or } \text{Ta}_3 \text{N}_5 \rightarrow 3 \text{ TaN} + \text{N}_2$).

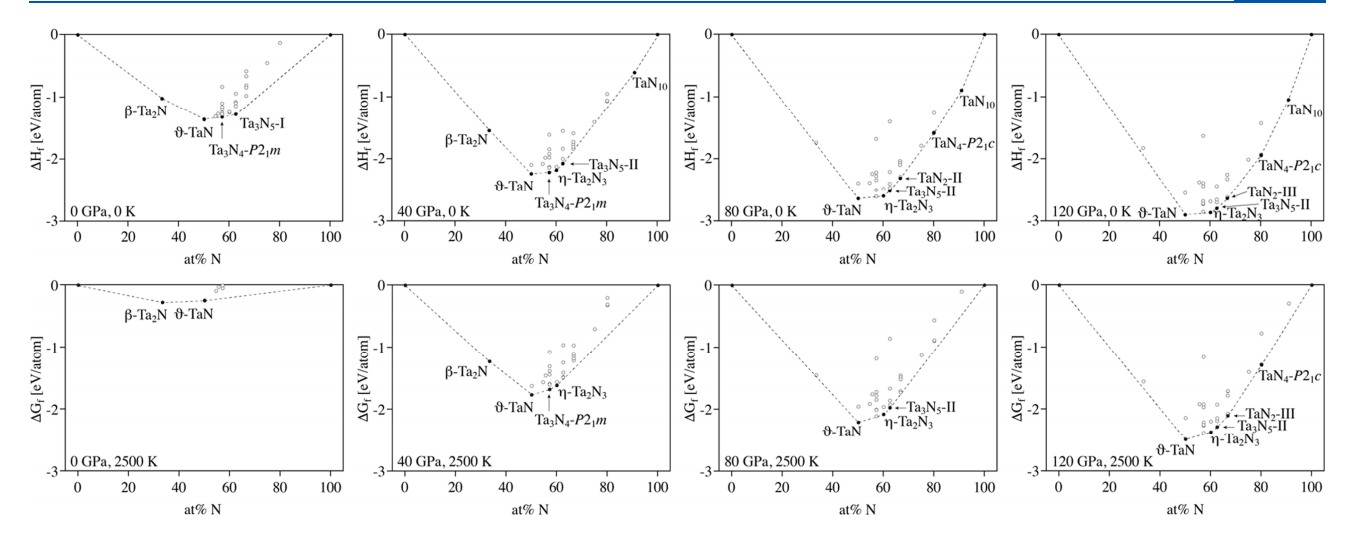


Figure 3. Convex hulls for the Ta–N system at 0, 40, 80, and 120 GPa. The top row refers to formation enthalpy (ΔH , in eV/atom). The bottom row refers to formation Gibbs energy (ΔG , in eV/atom) at 2500 K applying the moderate extrapolation given in Table 2. Phases stable against decomposition into any of its neighboring phases are indicated by the filled black dots as well as by their structure name (see also legend in Figure 2). For the various compositions nitrogen contents are given (in atom %): Ta (0), Ta₂N (33), TaN (50), Ta₅N₆ (55), Ta₄N₅ (56), Ta₃N₄ (57), Ta₂N₃ (60), Ta₃N₅ (63), TaN₂ (67), TaN₃ (75), TaN₄ (80), TaN₁₀ (91), and N₂ (100).

We show convex hulls based on enthalpy and based on Gibbs energy at 2500 K for different pressures in Figure 3. For the latter approach, we augment the enthalpy of nitrogen by the chemical potential change according to the moderate extrapolation for the fugacity of nitrogen as given in Table 2. Note that we use the same data as in Figures 1 and 2 but only present it in different ways. All convex hulls refer to the formation from the elements, $n \cdot \text{Ta} + m \cdot 1/2\text{N}_2 \rightarrow \text{Ta}_n \text{N}_m$. The most noticeable difference between the diagrams based on enthalpy and on Gibbs energy is that nitrogen-rich phases appear on the latter only at very high pressure and are noticeably absent at low pressures. This is simply a consequence of the molecular nitrogen having significantly lower chemical potential at elevated temperatures. Thus, Ta₃N₄ and Ta₂N₃ appear on the enthalpy-based convex hull at 0 GPa, while they both do not appear in the corresponding diagram based on Gibbs energy at 2500 K. Another example is TaN₁₀, which appears on the enthalpy-based convex hull at 40 GPa. However, this phase does not appear at 2500 K even at 120 GPa on the convex hull based on Gibbs energy. A convex hull based on Gibbs energy has yet another helpful characteristic: the most nitrogen-rich phase appearing on it is also the thermodynamically most stable one at the given conditions in the presence of excess nitrogen. Hence, it correctly predicts the outcome of DAC experiments at the applied temperature and pressure conditions, if nitrogen is used as the reactant and pressure medium.

DISCUSSION

Our assessment of the tantalum—nitrogen phase diagram at high temperature and high pressure targets the chemical synthesis of new compounds in state-of-the-art laser-heated diamond-anvil experiments that use nitrogen as the reactant and as pressure medium. The approach is a practical guide that augments quantum-chemical calculations with thermochemical data. For every Ta-N phase system, it yields a Gibbs energy surface in the pressure—temperature space. The tantalum—nitrogen *p*, *T*-phase diagram then identifies for every *p*, *T*-condition the one thermodynamically most stable phase and its

structure in the presence of excess nitrogen (see Figure 1). This information in itself is most helpful but applies to ideal conditions (homogeneous isotropic system and infinite time to establish equilibrium). In a real experiment, conditions vary at different locations of the reaction zone and kinetics do play a significant role. Hence, the manifold of alternative structures, some of which—under peculiar circumstances—may form as well, is also of interest. This manifold is explored by appropriate slices into the phase diagram made at constant pressure or at constant temperature (see Figure 2). Gibbs energy differences may be interpreted similar to a statistical weight, indicating the likelihood of a structure to emerge. Using the slices then also offers the opportunity to locate optimum experimental conditions to realize a particular structure in its stability field.

Calculations of a convex hull relying on relative enthalpies can serve as a guideline for experimentalists. However, such measures refer to 0 K only and have limited fidelity in predicting the synthesis of compounds with high nitrogen content given the substantial decrease of the chemical potential of nitrogen by -1.2 to -2.8 eV (per N atom) for 1000-3000K at 0 GPa. Even at pressures of 40 or 80 GPa, the chemical potential of nitrogen is lowered by -0.4 to -1.2 eV (per N atom) at 2000-3000 K, respectively, relative to its enthalpy. Computing convex hulls at different temperatures and pressures by augmenting the enthalpy of nitrogen with chemical potential change resolves this issue and enhances the fidelity in predictions. Convex hulls based on Gibbs energy also have the characteristic to readily identify the thermodynamically most stable structure at the given pressure and temperature in the presence of excess nitrogen.

In this study, we presented the data only for results using the SCAN functional. Calculations using the generalized-gradient-approximation (GGA) in the form of the Perdew–Burke–Ernzerhof (PBE) functional vield similar but not identical results. Enthalpy differences vary by up to 5 meV per atom and have the impact that ε -TaN and Ta₅N₆ do not appear in the convex hull, in contrast to previous calculations. For comparison with experimental data, we stress that in all

calculations we consider perfect ideal crystals only, while the nature of defects in a solid and its surface chemistry have an additional impact on the Gibbs energy. Additionally, the pathways and kinetics of decomposition or formation reactions or uneven reaction conditions may yield transient metastable intermediates or byproducts in an experiment.^{26,41}

A critical ingredient for our calculations is the assessment of the chemical potential of nitrogen at high temperature and high pressure. 18 Detailed experimental studies are needed and will further help to refine the analytical model. Previous highpressure experiments in the Ta-N system by Zerr et al. and Friedrich et al. operated with pressures between 15 and 27 GPa and temperatures around 2000 K.^{24,25} This is well in the stability range of η -Ta₂N₃ when using either the perfect gas or moderate extrapolation approach for the chemical potential change of nitrogen. The experiments, thus, render the progressive extrapolation less likely in this pressure range. A special consideration is needed for the experiments by Salamat et al.²⁶ Loading a diamond-anvil cell (DAC) with an amorphous polymeric N-rich Ta-N precursor, which at ambient pressure could also be crystallized to yield the ambient pressure modification Ta₃N₅-I, they increased the pressure to 20 GPa and performed laser heating for several minutes at 1500-2000 K. Subsequent XRD characterization at ambient temperature indicated a pressure of 22 GPa in the cell. The powder pattern of the product was analyzed to contain a phase assemblage of Ta₃N₅-II and the U₃Se₅-type of Ta₃N₅ together with small amounts of η -Ta₂N₃ and ε -N₂. We reason, based on the computed thermochemical data, that the second major component in the product besides Ta₃N₅-II is Ta₃N₅-III rather than the U₃Se₅-type. Indeed, at 22 GPa, the orthorhombic (Pmmn) structure of Ta₃N₅-III is -0.15 eV/ Ta₃N₅ more favorable than Ta₃N₅-II, while the U₃Se₅-type is 0.42 eV/Ta₃N₅ less favorable than Ta₃N₅-II. The two structures, Ta₃N₅-III and U₃Se₅-type, also have similar lattice parameters at 22 GPa (one parameter of Ta₃N₅-III is just half of one of the U₃Se₅-type). Note that Salamat et al. were not aware of a Ta₃N₅-III structure at the time of their analysis. The broad lines of their experimental powder pattern, however, make a clear phase determination difficult, as had been pointed out by the authors as well. The simultaneous appearance of η - $\mathrm{Ta_2N_3}$ and $\varepsilon\text{-N_2}$ is further rationalized by thermochemical data. Based on enthalpy, the system $3/2 \cdot \eta$ -Ta₂N₃ + $1/4 \cdot \varepsilon$ -N₂ is favored by -0.04 eV/Ta₃N₅ relative to Ta₃N₅-II, but still less favorable than Ta₃N₅-III by +0.11 eV/Ta₃N₅. A possible formation of tetragonal Ta_2N_3 and ε - N_2 is penalized by +0.16 eV/Ta₃N₅ relative to Ta₃N₅-II. At 1500-2000 K, an assemblage of η -Ta₂N₃ and ε -N₂ drops by -0.1 to -0.3 eV due to the chemical potential change of nitrogen within the moderate extrapolation data. Hence, the experimental conditions chosen by Salamat et al. are close to the phase boundary between Ta₃N₅-III and η-Ta₂N₃, which is also reflected in Figure 1 (middle). Clever choice of an N-rich precursor and slow kinetics at lower temperatures in comparison to the experiments carried out by Friedrich et al. may further help in attaining Ta₃N₅ polymorphs. Thus, the experiments of Salamat et al. give credibility to the moderate extrapolation data for the chemical potential change of nitrogen but do not fully exclude a more perfect gas behavior.

To synthesize pure Ta₃N₅-II within its large stability field in the p, T-phase diagram, experimentalists can choose optimum conditions of 2500 K and 80 GPa, assuming the moderate extrapolation for nitrogen fugacity to hold. Such pressures and

temperatures are not uncommon and have been applied in recent experiments.⁵⁻⁷ Besides, more fascinating Ta-N polymorphs are attainable at even higher pressures, the mixed nitride-per-nitrides of TaN_2 (= $Ta_2N_2(N_2)$) between 93 and 116 GPa, and TaN_4 with its polyatomic N_8^{10-} -anion at pressures beyond.

CONCLUSIONS

We provide a practical and comprehensive approach to work out pressure-temperature phase diagrams. It combines density functional theory computations with thermodynamic calculations and includes proposed data for the chemical potential of nitrogen at high pressure and high temperature. Applying the method to the tantalum-nitrogen system, we receive a phase diagram for pressures up to 140 GPa and temperatures between 1000 and 4000 K. The phase diagram identifies stability fields of Ta-N structures in the presence of excess nitrogen, therefore, under conditions typical to state-of-the-art DAC experiments. Optimum conditions with the maximum driving force for successful syntheses are found by slicing the phase diagram at constant pressure or at constant temperature. Our results allow us not only to account for the outcome of recent high-pressure experiments that synthesized new Ta-N polymorphs but also to predict p, T-conditions necessary to synthesize the proposed Ta₂N₂(N₂) and Ta₂N₈. Overall, much data computed in recent years can be brought to more use for experimentalists with this method.

AUTHOR INFORMATION

Corresponding Author

Peter Kroll - Department of Chemistry and Biochemistry, The University of Texas at Arlington, Arlington, Texas 76019, *United States;* orcid.org/0000-0003-4782-2805; Email: pkroll@uta.edu

Author

Hanof Alkhaldi - Department of Chemistry and Biochemistry, The University of Texas at Arlington, Arlington, Texas 76019, *United States*; orcid.org/0000-0002-6478-1438

Complete contact information is available at: https://pubs.acs.org/10.1021/acs.jpcc.0c04143

The authors declare no competing financial interest.

ACKNOWLEDGMENTS

This work was supported by the National Science Foundation (NSF) through award OISE-1743701. The computational work was made possible through generous grants by the Texas Advanced Computing Center in Austin, TACC, Texas, and by the High Performance Computing facilities at UTA. H.A. acknowledges support by the Government of Saudi Arabia.

REFERENCES

- (1) Salamat, A.; Hector, A. L.; Kroll, P.; McMillan, P. F. Nitrogen-Rich Transition Metal Nitrides. Coord. Chem. Rev. 2013, 257, 2063-
- (2) Zerr, A.; Miehe, G.; Riedel, R. Synthesis of Cubic Zirconium and Hafnium Nitride Having Th₃P₄ Structure. Nat. Mater. 2003, 2, 185-
- (3) Crowhurst, J. C.; Goncharov, A. F.; Sadigh, B.; Evans, C. L.; Morrall, P. G.; Ferreira, J. L.; Nelson, A. J. Synthesis and

- Characterization of the Nitrides of Platinum and Iridium. Science **2006**, 311, 1275-1278.
- (4) Niwa, K.; Fukui, R.; Terabe, T.; Kawada, T.; Kato, D.; Sasaki, T.; Soda, K.; Hasegawa, M. High-Pressure Synthesis and Phase Stability of Nickel Pernitride. Eur. J. Inorg. Chem. 2019, 2019, 3753-3757.
- (5) Bykov, M.; et al. High-Pressure Synthesis of Ultraincompressible Hard Rhenium Nitride Pernitride Re₂(N₂)(N)2 Stable at Ambient Conditions. Nat. Commun. 2019, 10, No. 2994.
- (6) Bykov, M.; Khandarkhaeva, S.; Fedotenko, T.; Sedmak, P.; Dubrovinskaia, N.; Dubrovinsky, L. Synthesis of FeN₄ at 180 GPa and Its Crystal Structure from a Submicron-Sized Grain. Acta Crystallogr., Sect. E: Crystallogr. Commun. 2018, 74, 1392.
- (7) Bykov, M.; et al. Fe-N System at High Pressure Reveals a Compound Featuring Polymeric Nitrogen Chains. Nat. Commun. 2018, 9, No. 2756.
- (8) Bassett, W. A. Diamond Anvil Cell, 50th Birthday. High Pressure Res. 2009, 29, 163-186.
- (9) Boehler, R. Laser Heating in the Diamond Cell: Techniques and Applications. Hyperfine Interact. 2000, 128, 307-321.
- (10) Eremets, M. I.; Gavriliuk, A. G.; Trojan, I. A.; Dzivenko, D. A.; Boehler, R. Single-Bonded Cubic Form of Nitrogen. Nat. Mater. 2004, 3, 558-563.
- (11) Pickard, C. J.; Needs, R. J. Ab Initio Random Structure Searching. J. Phys.: Condens. Matter 2011, 23, No. 053201.
- (12) Oganov, A. R.; Ma, Y. M.; Lyakhov, A. O.; Valle, M.; Gatti, C. Evolutionary Crystal Structure Prediction as a Method for the Discovery of Minerals and Materials In Theoretical and Computational Methods in Mineral Physics: Geophysical Applications; Wentzcovitch, R.; Stixrude, L., Eds.; 2010; Vol. 71, pp 271-298.
- (13) Lonie, D. C.; Zurek, E. Xtalopt: An Open-Source Evolutionary Algorithm for Crystal Structure Prediction. Comput. Phys. Commun. 2011, 182, 372-387.
- (14) Wang, Y. C.; Lv, J. A.; Zhu, L.; Ma, Y. M. Crystal Structure Prediction Via Particle-Swarm Optimization. Phys. Rev. B 2010, 82, No. 094116.
- (15) Kroll, P. Hafnium Nitride with Thorium Phosphide Structure: Physical Properties and an Assessment of the Hf-N, Zr-N, and Ti-N Phase Diagrams at High Pressures and Temperatures. Phys. Rev. Lett. 2003, 90, No. 125501.
- (16) Kroll, P.; Schröter, T.; Peters, M. Prediction of Novel Phases of Tantalum(V) Nitride and Tungsten(VI) Nitride That Can Be Synthesized under High Pressure and High Temperature. Angew. Chem., Int. Ed. 2005, 44, 4249-4254.
- (17) Sun, W. H.; Holder, A.; Orvananos, B.; Arca, E.; Zakutayev, A.; Lany, S.; Ceder, G. Thermodynamic Routes to Novel Metastable Nitrogen-Rich Nitrides. Chem. Mater. 2017, 29, 6936-6946.
- (18) Alkhaldi, H.; Kroll, P. Chemical Potential of Nitrogen at High Pressure and High Temperature: Application to Nitrogen and Nitrogen-Rich Phase Diagram Calculations. J. Phys. Chem. C 2019, 123, 7054-7060.
- (19) Jiang, C.; Lin, Z. J.; Zhao, Y. S. Thermodynamic and Mechanical Stabilities of Tantalum Nitride. Phys. Rev. Lett. 2009, 103, No. 185501.
- (20) Zhang, J.-D.; Wang, H.-F. First-Principles Calculations of Structural and Electronic Properties of Ta2N3 under High Pressures. Phys. B 2013, 428, 89-93.
- (21) Li, D.; Tian, F. B.; Duan, D. F.; Bao, K.; Chu, B. H.; Sha, X. J.; Liu, B. B.; Cui, T. Mechanical and Metallic Properties of Tantalum Nitrides from First-Principles Calculations. RSC Adv. 2014, 4, 10133-10139.
- (22) Weinberger, C. R.; Yu, X. X.; Yu, H.; Thompson, G. B. Ab Initio Investigations of the Phase Stability in Group IVb and Vb Transition Metal Nitrides. Comput. Mater. Sci. 2017, 138, 333-345.
- (23) Xing, W. D.; Wei, Z. J.; Yu, R.; Meng, F. Y. Prediction of Stable High-Pressure Structures of Tantalum Nitride TaN2. J. Mater. Sci. Technol. 2019, 35, 2297-2304.
- (24) Zerr, A.; et al. High-Pressure Synthesis of Tantalum Nitride Having Orthorhombic U₂S₃ Type Structure. Adv. Funct. Mater. 2009, 19, 2282-2288.

(25) Friedrich, A.; Winkler, B.; Bayarjargal, L.; Arellano, E. A. J.; Morgenroth, W.; Biehler, J.; Schroder, F.; Yan, J. Y.; Clark, S. M. In Situ Observation of the Reaction of Tantalum with Nitrogen in a Laser Heated Diamond Anvil Cell. J. Alloys Compd. 2010, 502, 5-12.

pubs.acs.org/JPCC

- (26) Salamat, A.; Woodhead, K.; Shah, S. I. U.; Hector, A. L.; McMillan, P. F. Synthesis of U₃Se₅ and U₃Te₅ Type Polymorphs of Ta₃N₅ by Combining High Pressure-Temperature Pathways with a Chemical Precursor Approach. Chem. Commun. 2014, 50, 10041-
- (27) Hohenberg, P.; Kohn, W. Inhomogeneous Electron Gas. Phys. Rev. 1964, 136, B864-B871.
- (28) Kresse, G. Ab-Initio Molecular-Dynamics for Liquid-Metals. J. Non-Cryst. Solids 1995, 192-193, 222-229.
- (29) Kresse, G.; Hafner, J. Ab-Initio Molecular-Dynamics Simulation of the Liquid-Metal Amorphous-Semiconductor Transition in Germanium. Phys. Rev. B 1994, 49, 14251-14269.
- (30) Kresse, G.; Furthmüller, J. Efficiency of Ab-Initio Total Energy Calculations for Metals and Semiconductors Using a Plane-Wave Basis Set. Comput. Mater. Sci. 1996, 6, 15-50.
- (31) Blöchl, P. E. Projector Augmented-Wave Method. Phys. Rev. B **1994**, *50*, 17953-17979.
- (32) Kresse, G.; Joubert, D. From Ultrasoft Pseudopotentials to the Projector Augmented-Wave Method. Phys. Rev. B 1999, 59, 1758-
- (33) Sun, J. W.; Ruzsinszky, A.; Perdew, J. P. Strongly Constrained and Appropriately Normed Semilocal Density Functional. Phys. Rev. Lett. 2015, 115, No. 036402.
- (34) Kroll, P. Advances in Computation of Temperature-Pressure Phase Diagrams of High-Pressure Nitrides. Key Eng. Mater. 2008, 403,
- (35) Zhao, Z. L.; Bao, K.; Tian, F. B.; Duan, D. F.; Liu, B. B.; Cui, T. Phase Diagram, Mechanical Properties, and Electronic Structure of Nb-N Compounds under Pressure. Phys. Chem. Chem. Phys. 2015, 17, 22837-22845.
- (36) Kroll, P. Pathways to Metastable Nitride Structures. J. Solid State Chem. 2003, 176, 530-537.
- (37) Jacobsen, R. T.; Stewart, R. B.; Jahangiri, M. Thermodynamic Properties of Nitrogen from the Freezing Line to 2000-K at Pressures to 1000-MPa. J. Phys. Chem. Ref. Data 1986, 15, 735-909.
- (38) Strähle, J. Die Kristallstruktur des Tantal(V)-Nitrids Ta3N5. Z. Anorg. Allg. Chem. 1973, 402, 47-57.
- (39) Zhang, J.; Oganov, A. R.; Li, X. F.; Niu, H. Y. Pressure-Stabilized Hafnium Nitrides and Their Properties. Phys. Rev. B 2017, 95, No. 020103(R).
- (40) Perdew, J. P.; Burke, K.; Ernzerhof, M. Generalized Gradient Approximation Made Simple. Phys. Rev. Lett. 1996, 77, 3865-3868.
- (41) Bhadram, V. S.; Liu, H. Y.; Xu, E. S.; Li, T. S.; Prakapenka, V. B.; Hrubiak, R.; Lany, S.; Strobel, T. A. Semiconducting Cubic Titanium Nitride in the Th₃P₄ Structure. Phys. Rev. Mater. 2018, 2, No. 011602(R).